Journal of Renewable Materials
DOI:10.32604/jrm.2020.010558
Article

Tech Science Press

Interfacial Modification of Corn Stalk Cellulose Reinforced Used Rubber Powder Composites Treated with Coupling Agent

Weili Wu* **and Fengyu Chen**

College of Materials Science and Engineering, Qiqihar University, Qiqihar, 161006, China
*Corresponding Author: Weili Wu. Email: wuweili2001@163.com
Received: 10 March 2020; Accepted: 06 May 2020

Abstract: Corn stalk cellulose (CS)/used rubber powder (RP) composites were prepared by mixing, the silane coupling agent 3-Mercaptopropyl trimethoxysilane (KH590), r-Aminopropyltrieth oxysilane (KH550), isopropyl dioleic (dioctylphosphate) titanate (HY101) and bis-(γ-triethoxysilylpropyl)- tetrasulfide (Si69) were used to modify the interface of composites. The effects of the CS and coupling agents on the mechanical properties, thermal properties, interfacial morphology and structure of the composites were investigated, respectively. The results showed that the addition of CS could effectively improve the mechanical properties of the composites. Compared with the untreated composites, the interfacial bonding between CS and RP was significantly improved by the coupling modification treatment, and the tensile strength and elongation at break of composites with Si69 increased by 3.13 MPa and 10%, respectively, the Si69 showed the best coupling modification effect, followed by KH590, then KH550 and HY101 when the CS content was 25 pph (part per hundred) and coupling agent 1.5 pph, and the thermal decomposition temperature increased by 30°C.

Keywords: Corn stalk cellulose; used rubber powder; composites; modification

1 Introduction

In recent years, with the shortage of resources and the increasingly serious environmental problems, the comprehensive utilization of biodegradable materials and waste has become one of the hottest research directions in the material industry [1]. As the automobile industry develops rapidly, the more and more waste tires have become a hot issue, and the waste rubber can be used instead of rubber material, such as in road materials, and the field of low demand for the rubber. Therefor the used tires were changed into rubber powder of various sizes to broaden its application field and made used rubber powder (RP) become new black gold [2–4]. It can be applied in the building materials, road materials, modified asphalt, cement [5,6], dam, roof waterproofing coating, building caulking, linoleum, and insulating filler in the construction aspects such as thermal insulating material [7–9]. The RP was a thermosetting polymer with a certain amount of unsaturated bonds and still has some excellent properties of rubber, such as elasticity, toughness, wear resistance and anti-slip, so it has been widely used as reinforcement materials and fillers [10–12]. However, it is restricted to apply alone due to the poor mechanical properties of the RP [13,14]. Cellulose has many excellent properties [15], so chosen to reinforce RP.

However, it was found that the corn stalk contained a large number of natural fiber, with high strength, low density, large specific area and length to diameter ratio, so the corn stalk cellulose (CS) not only used as reinforcement materials, but also have heat preservation, heat insulation performance [16,17]. As a result, the CS was selected as the reinforcement material to improve the mechanical properties of the RP matrix and broadened its application scope. However, due to the existence of a large number of hydrophilic hydroxyl in the corn stalk, it decreased with the interfacial compatibility between hydrophobic RP and CS. Therefore, the interface compatibility between them must be improved, it had become a main research direction [18]. In this work, we would use four kinds of different coupling agents (silane coupling agent KH550, KH590, Si69 and titanate coupling agent HY101), respectively, modified the surface of the composites, and studied the effect of CS content on the structure and properties of composites to prepare green CS/RP composites. It would partly replace the boards with low strength requirements, such as the insulation board in the middle of the wall, partition plate, middle layer of the composite board and parking floor and so on.

2 Materials and Methods

2.1 Materials

Used tire rubber powder (RP) which is mainly made of waste tire (China, Heilongjiang), with diameter of 0.10–0.32 mm and particle size of 10 orders, its main composition is natural rubber, butadiene rubber and styrene butadiene rubber. Corn stalk cellulose (CS) was collected by Qiqihar field (China, Heilongjiang), in filamentous shape with diameter of 0.5–1 mm, average fiber length of 20 mm. Titanate coupling agent HY101 as industry product (isopropyl dioleic (dioctyl phosphate) titanate, $C_{55}H_{111}O_9Ti$) was supplied by Huaian Heyuan chemical Ltd., (China, Jiangsu). KH590 ((3-Mercaptopropyl) trimethoxysilane, HS $(CH_2)_3Si(OCH_3)_3$), KH550 (r-Aminopropyltrieth oxysilane, $H_2NCH_2CH_2CH_2Si(OC_2H_5)_3$) and Si69 (bis-(γ-triethoxysilylpropyl)-tetrasulfide, $(H_5C_2O)_3Si\ (CH_2)_3{\cdot}S_4{\cdot}(CH_2)_3{\cdot}Si(OC_2H_5)_3$) were supplied by Nanjing Aocheng Chemical Ltd., (China, Jiangsu) as industry product. The other ingredients were all commercial materials on the market.

2.2 Preparation of Composites

The first step was the preparation of corn stalk silk. After washing and drying corn stalk in CS-700 high-speed multi-function crusher in crushing control time around 90 s, selected filamentous corn stalk about 20 mm in length, the corn stalk in the beaker containing NaOH solution soaked for 24 h, washed with deionized water twice for 3 h by a YM-020-S ultrasonic instrument, and dried for 1 h in a 202 electric heating oven, gotten activated CS. At last, the different silane coupling agents were diluted with anhydrous ethanol (the mass ratio of silane coupling agent and anhydrous ethanol was 1:6), and the diluted silane coupling agent was even sprayed on the CS with stirring.

The second step was the preparation of CS/RP composites. First, the RP of 100 g (pph, part per hundred), was mixed by adding 2.5 pph sulfur in a SK-160B double roll mixer, the roller temperature was 50–60°C, and the roller distance was 1.0 mm for 5 min, and the 25 pph CS treated with the silane coupling agent of 1.5 pph was mixed until the mixture was uniform at 50–60°C for 1–2 min, the distance between two rolls was 1–2 mm. Then the mixture was cured in an XLB-D350 plate vulcanizer at 150°C for 30 min under 5 MPa.

2.3 Characterization

The dumb-bell shaped rubber specimens were prepared from a sheet of the vulcanizates by cutting. The mechanical properties were tested by an electronic universal testing machine (model CSS-2200, Changchun Intelligent Instrument Equipment Ltd., China) with a strain rate of 300 mm min^{-1} according to ISO 37-2005. Shore A hardness was measured on 6 mm thick samples according to ISO 48-2018. Heat aging of the samples was measured at 150°C for 24 h according to ISO 188-2001. For

each of the measurements, an average of at least five readings was taken. The errors in the measurements of the mechanical properties were within 10%.

Vulcanization characteristics test were carried out by a Mooney viscosity meter (model JC-2000G, Jiangdu Jingcheng test instrument factory, China) at 120°C, the minimum torque (M_L) and maximum torque (M_H) and t_{90} was tested according to ISO289-1985.

The vulcanizate samples were fractured in liquid nitrogen, then the fracture surface was sputtered with gold, and the fracture morphologies of the samples were observed by scanning electron microscopy (SEM; model S-4300, Hitachi Co., Japan).

X-ray photoelectron spectroscopy (XPS) of the sample (2 × 2 × 1 mm^3) was recorded by using a ESCALAB250Xi X-ray photoelectron spectrometer (Thermo Co., America) with an aluminum (mono) Kα source (1486.6 eV). The aluminum Kα source was operated at 15 kV and 10 mA. All core level spectra were referenced to the C1s neutral carbon peak at 284.7 eV.

The infrared spectra of the samples were recorded using an IR-7685 Fourier transform infrared (FTIR) spectrometer (model Spectrum One, Perkin Elmer Co., America), FTIR spectra were collected after 256 scans at a resolution of 2 cm^{-1} in the region of 4000 to 500 cm^{-1}, at room temperature.

The samples of vulcanizates were cut into slices 5 × 5 × 1 mm^3 by a ZY-1025 manual sheet- punching machine (Jiangdu Changlong Experimental Machinery Factory, China), and the range of samples from 0 μm to 150 μm were observed by a infrared imager (Spotlight 400 Near Infrared Chemical Imager provided by the Perkin Elmer Co., Ltd., USA) to investigate the compatibility between CS and RP by absorbing light waves in the region of 4000–750 cm^{-1} at room temperature. The CS and RP absorbed light differently, their infrared image showed different color regions.

The thermo gravimetric analysis was performed using a thermogravimetric (TG) analyzer (model STA449F3, NETZSCH Co., Germany). The temperature of tests ranged from 0 to 650°C, with a heating rate of 5 °C/min.

3 Results and Discussion

3.1 Effect of CS Content on the Mechanical Properties of the CS/RP Composites

The effect of CS content on the mechanical properties of the CS/RP composites was studied in this work. With the addition of the CS, the tensile strength, elongation at break and Shore A hardness of the composites increased first and then decreased in Tab. 1. It could be explained that the CS contained a large number of natural fiber, the crack resistance effect of the fiber could prevent the growth and proliferation of tiny crack inside gelled material, improving the mechanical properties of the CS/RP composites [19]. When the CS content was over 25 pph, the excessive CS could lead to accumulation of CS, not evenly dispersed and covered by the CS, and thus the mechanical properties of CS/RP composites decreased. As is known to all, the mechanical properties of composites directly determined the service life of the product. In order to determine CS content, the mechanical properties of CS/RP composites after heat aging were also studied. It was found that the changes of mechanical properties before and after aging were large. When the CS content was 25 pph, the change of the composites' mechanical properties before and after heat aging was the smallest, it shown that the thermal properties of composites with CS of 25 pph were the best.

3.2 Effect of Coupling Agent on the Mechanical Properties of the Composites

It could be seen that the increase of the mechanical properties of RP was not obvious by adding CS in Tab. 1, the effect of different coupling agent on the mechanical properties of CS/RP composites was studied as shown in Tab. 2. No matter which coupling agent was used to treat CS, the tensile strength and elongation at break increased first and then decreased with the addition of coupling agent, but the change of Shore A hardness was very small. On the whole, Si69 showed the best coupling modification effect, followed by

Table 1: Effect of CS content on the mechanical properties of composites

CS content (pph)	Tensile strength (MPa) before/ after heat aging	Elongation at break (%) before/ after heat aging	Shore A hardness before/ after heat aging
0	1.80/0.89	23/20	60/66
10	1.97/1.04	27/21	69/74
15	1.99/1.13	28/21	70/75
20	2.03/1.26	28/22	71/76
25	2.15/1.75	31/26	72/77
30	2.03/1.32	28/24	71/76
35	1.98/1.15	25/22	71/76
40	1.88/1.07	24/21	69/74

Table 2: Effect of KH550, KH590, HY101 and Si69 content on the mechanical properties of the composites

Coupling agent content (pph)	KH550/KH590/HY101/Si69		
	Tensile strength (MPa)	Elongation at break (%)	Shore A hardness
0	2.15	31	72
0.5	4.10/4.18/4.17/4.58	31/32/31/33	73/73/73/73
1.0	4.17/4.33/4.26/4.92	31/33/32/36	73/73/73/74
1.5	4.17/4.38/4.37/5.28	34/34/32/41	7373/73/74
2.0	4.14/4.25/4.15/4.85	31/34/31/37	73/74/73/74
2.5	4.13/4.20/4.14/4.59	31/32/31/34	73/73/73/74

KH590, and then KH550 and HY101 in the CS/RP (25/100). When the Si69 of 1.5 pph was used, the effect was the best, and the tensile strength increased by 3.13 MPa, elongation at break increased by 10%, and the Shore A hardness was almost no change.

It has been attributed to Si69 structure, the sulfur (-S4-) in silane coupling agent Si69 played a bridge role [20], coupling CS to RP, the silanol of Si69 could react with the dehydrate of the CS and form hydrogen bond at one end, and the other end combined with RP to form strong covalent bond, so the RP and CS formed the crosslinked network by adding Si69, the mechanism was shown in Fig. 1. And other coupling agents had not Si69 effect, so the mechanical properties of the composites treated with Si69 were better than those of the other composites.

At the same time, the infrared spectra of CS/RP composites treated with Si69 coupling agent were shown in Fig. 2. The curve of CS/RP composites treated with Si69 showed a symmetrical absorption peak of -CH in 2857.40 cm^{-1}, while no symmetrical absorption peak appeared in the curves of RP, CS and Si69. When the CS/RP composites was treated with Si69, the vibration absorption peak of -C=O appeared at 1729.01 cm^{-1}, and new absorption peaks of CH_2, Si-O-Si and Si-O-C appeared at 1240 cm^{-1}, 840 cm^{-1} and 711.68 cm^{-1}, respectively. The presence of Si-O-Si and Si-O-C absorption peak meant that there were chemical reaction between CS and RP treated with the coupling agent Si69. It further proved that coupling agent Si69 could improve the mechanical properties of CS/RP composites.

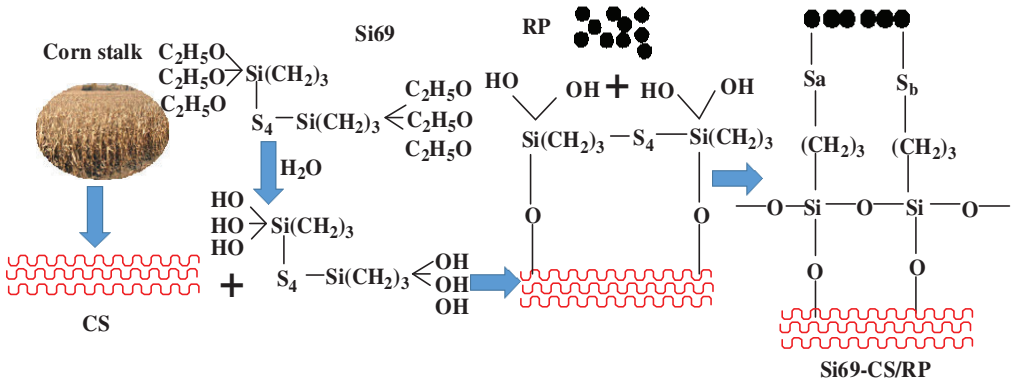

Figure 1: Reaction mechanism of CS/RP composites treated with Si69

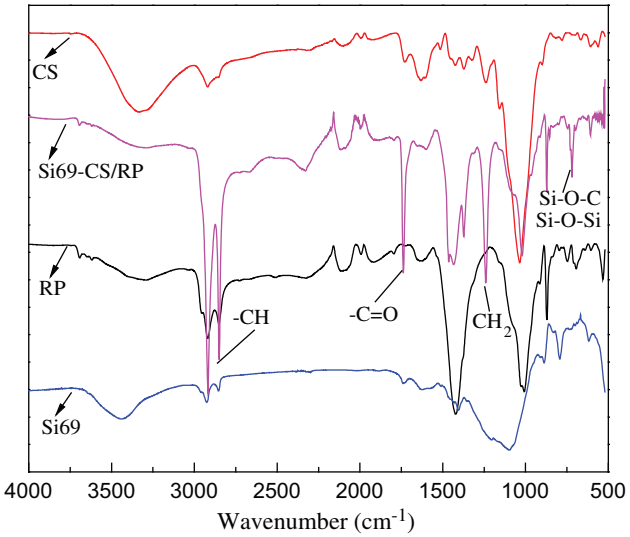

Figure 2: IR spectra of CS/RP composites with Si69

3.3 Effect of Coupling Agent Si69 on the Curing Characteristics

In order to determine the effect Si69 on the CS/RP composites, the curing characteristics of CS/RP composites were studied as shown in Tab. 3. The addition of silane coupling agent Si69 reduced the time t_{10} and t_{90}, and increased the maximum torque M_H and minimum torque M_L. This was mainly attributed to the RP (mainly natural rubber, butadiene rubber and styrene butadiene rubber as well as the mixture of filler). If the sulfur (S) was only used, the S in RP played the role of cross-linking. However, the addition of Si69 cured RP more fully, and Si69 decomposed into curing accelerator to shorten the burning time. At the same time, the special structure of Si69 (containing 4 S atoms) could participate in the curing process and increase the torque. From the aspects of curing effect, production processing and application, it was also determined that the curing effect of Si69-CS/ RP was better than that of CS/RP composites.

3.4 Effect of Coupling Agent Si69 on the Interface Morphology and Structure of the Composites

The CS with Si69 in the dispersion of RP could be proved by their SEM and infrared phase diagrams. In Fig. 3, the CS treated with Si69 was closely combined with RP, and the distribution of CS in the RP was uniform and there was no gap, so the compatibility of CS/RP composites treated with Si69 was better.

Table 3: Effect of Si69 on the curing characteristics of CS/RP composites

Typle	t_{10} (s)	t_{90} (s)	M_H (dN m)	M_L (dN m)	M_H-M_L (dN m)
RP	128	1219	38.62	3.93	34.69
CS/RP	104	1083	40.02	5.09	34.93
Si69-CS/RP	85	780	59.51	6.93	53.58

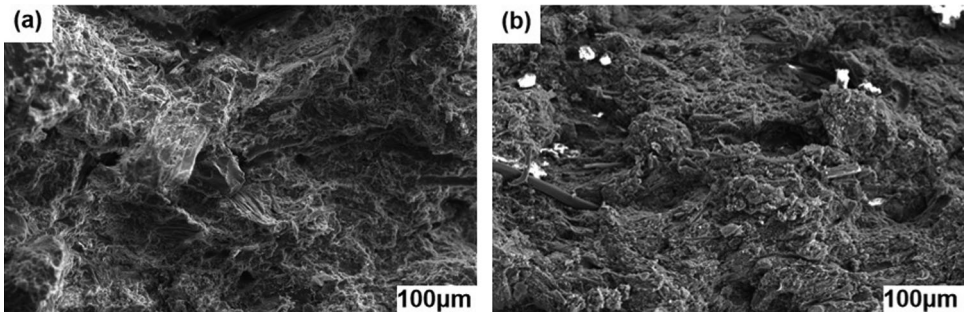

Figure 3: SEM images of (a) Si69-CS/RP and (b) CS/RP

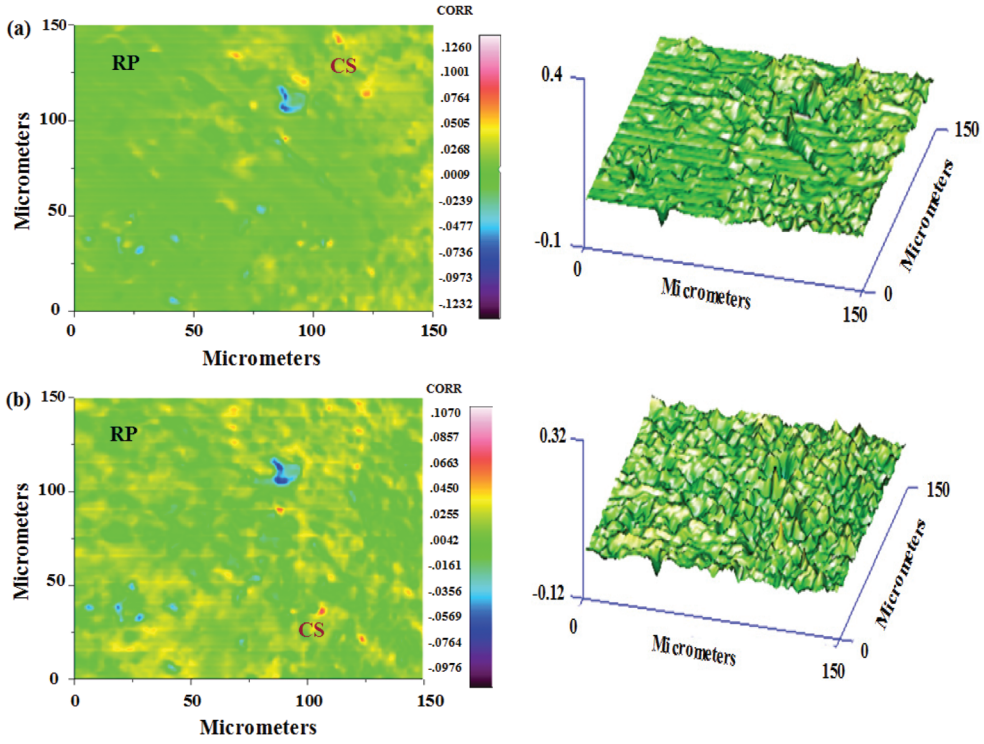

Figure 4: Infrared thermal images of (a) CS/RP and (b) Si69-CS/RP composites

As can be seen from Fig. 4, CS and RP were cross-linked after the modification of Si69, CS could be more evenly dispersed in the RP, and the infrared phase diagram of CS/RP composites was uniform. However, the CS was not evenly dispersed in the RP without Si69, and the accumulation of CS was obvious, indicating that the dispersion of CS in the RP was poor.

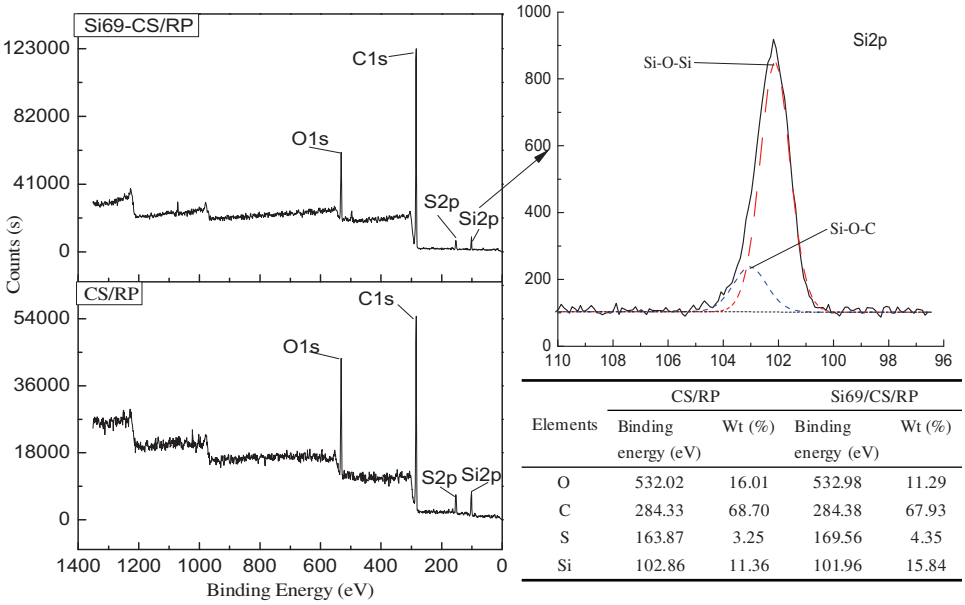

Elements	CS/RP		Si69/CS/RP	
	Binding energy (eV)	Wt (%)	Binding energy (eV)	Wt (%)
O	532.02	16.01	532.98	11.29
C	284.33	68.70	284.38	67.93
S	163.87	3.25	169.56	4.35
Si	102.86	11.36	101.96	15.84

Figure 5: XPS spectra of CS/RP composites with Si69 coupling agent

In order to understand the composition structure of CS/RP composites, X-ray photoelectron spectroscopy (XPS) of CS/RP composites was tested as shown in Fig. 5. The CS/RP composites without and with coupling agent Si69 contained O1s, C1s, S2p and Si2p. C1s and O1s elements were from the RP, S2p and Si2p elements were from sulfur and silica filler (hydrated silicon dioxide), and O1s element was from the cellulose, hemicellulose and lignin of CS, the CS cellulose was composed of D-pyran glucose (carbon, hydrogen and oxygen elements). After the addition of coupling agent Si69, CS/RP still contained these four elements, but the difference was that contained more elements Si and S, which was consistent with the chemical composition of the coupling agent Si69 ($(H_5C_2O)3Si\ (CH_2)_3{\cdot}S_4{\cdot}(CH_2)_3Si(OC_2H_5)_3$). The content and binding energy of elements Si and S were changed with adding Si69, which was due to the fact that the coupling agent Si69 was used as a bridge to connect the rubber and CS, it could be certified from the Si2p sub-peak. Si2p has two sub-peaks of Si-O-Si and Si-O-C, the former was considered as the peak of silica, and the latter peak was generated by Si69 and RP coupling. This also proved the infrared results from the side, that is, Si69 and CS/RP took place chemical reaction to improve the compatibility between CS and RP.

3.5 Effect of Si69 on Thermal Properties of CS/RP Composites

The mechanical properties and dispersion of Si69 modified CS/RP composites were better, and the thermal stability of Si69 modified CS/RP composites was also studied in this work as shown in Fig. 6. The thermal stability of pure RP was slightly better than that of CS/RP composites and Si69 modified CS/RP composites in Fig. 6a, in addition, the RP curve had more thermal stability in 500–600°C than CS/RP and Si69 composites as the residue was 43, 39, and 37% respectively. It could be explained that thermal stability of CS was poor, the CS has been carbonized and decomposed at 450°C, that was why the thermal stability of CS/RP and Si69 modified CS/RP composites was lower. And the Si69-CS/RP composites started to decompose in a small amount at 160°C and gradually decomposite at 200°C, this thermal decomposition did not affect use and process of composites. It could be seen that the Si69 modified composites could inhibit the decomposition rate in Fig. 6b, the modified composites reached decomposition peak for the first time at about 290°C, and unmodified composites reached decomposition

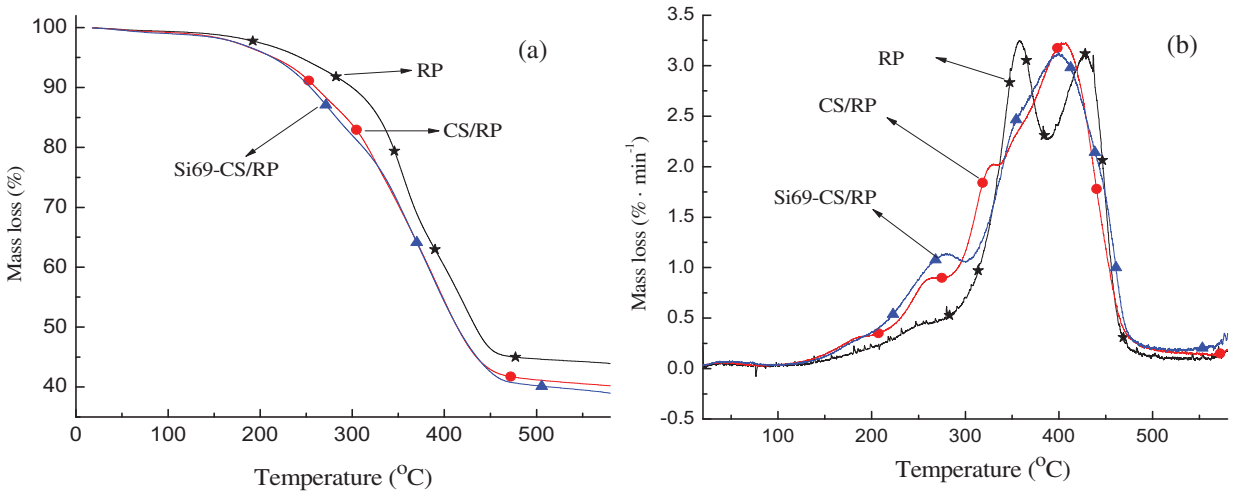

Figure 6: Thermogravimetric curves of (a) TG and (b) DTG

peak for the first time at about 260°C, it illustrated that the thermal stability of Si69 modified CS/RP composites was better than that of the unmodified composites within the service range temperature.

4 Conclusion

In the present study CS/RP composites were prepared by adding four kinds of coupling agents to modify the interface of composites and reinforce CS/RP composites. When the CS of 25 pph and Si69 of 1.5 pph were added into RP, the mechanical properties of Si69-CS/RP composites were the best, the tensile strength and elongation at break of composites with Si69 increased by 3.13 MPa and 10%, respectively, followed by KH590, then KH550 and HY101. The compatibility and thermal stability of Si69 modified CS/RP composites were improved, and the thermal decomposition temperature was increased 30°C compared with the CS/RP composites.

Funding Statement: This work was supported by 2019 Science and Graduate Innovative Research Project of Qiqihar University Heilongjiang Province, China (YJSCX2019060).

Conflicts of Interest: The authors declare that they have no conflicts of interest to report regarding the present study.

References

1. Gopi, S., Pius, A., Thomasbc, S. (2016). Enhanced adsorption of crystal violet by synthesized and characterized chitin nano whiskers from shrimp shell. *Journal of Water Process Engineering, 14,* 1–8. DOI 10.1016/j.jwpe.2016.07.010.
2. Zhang, Z. X., Zhang, S. L., Lee, S. H., Kang, D. J., Bang, D. S. et al. (2008). Microcellular foams of thermoplastic vulcanizates (TPVs) based on waste ground rubber tire powder. *Materials Letters, 62(28),* 4396–4399. DOI 10.1016/j.matlet.2008.07.039.
3. Sienkiewicz, M., Janik, H., Borzedowska-Labuda, K., Kucinska-Lipka, J. (2017). Environmentally friendly polymer-rubber composites obtained from waste tyres: a review. *Journal of Cleaner Production, 147,* 560–571. DOI 10.1016/j.jclepro.2017.01.121.
4. Gopi, S., Kargl, R., Kleinschek, K. S., Pius, A., Thomas, S. (2018). Chitin nanowhisker–inspired electrospun PVDF membrane for enhanced oil-water separation. *Journal of Environmental Management, 228,* 249–259. DOI 10.1016/j.jenvman.2018.09.039.

5. Girskas, G., Nagrockien, D. (2017). Crushed rubber waste impact of concrete basic properties. *Construction and Building Materials, 140,* 36–42. DOI 10.1016/j.conbuildmat.2017.02.107.
6. Hassim, D. H., Abang, I., Abraham, F., Summerscales, J., Brown, P. (2019). The effect of interface morphology in waste tyre rubber powder filled elastomeric matrices on the tear and abrasion resistance. *Express Polymer Letters, 13(3),* 248–260. DOI 10.3144/expresspolymlett.2019.21.
7. Saberi, K. F., Fakhri, M., Azami, A. (2017). Evaluation of warm mix asphalt mixtures containing reclaimed asphalt pavement and crumb rubber. *Journal of Cleaner Production, 165,* 1125–1132. DOI 10.1016/j.jclepro.2017.07.079.
8. Thomas, B. S., Gupta, R. C. (2016). A comprehensive review on the applications of waste tire rubber in cement concrete. *Renewable and Sustainable Energy Reviews, 54,* 1323–1333. DOI 10.1016/j.rser.2015.10.092.
9. Liang, M., Xin, X., Fan, W. Y., Sun, H. D., Yao, Y. et al. (2015). Viscous properties, storage stability and their relationships with microstructure of tire scrap rubber modified asphalt. *Construction and Building Materials, 74,* 124–131. DOI 10.1016/j.conbuildmat.2014.10.015.
10. Aoudia, K., Azem, S., Hocine, N. A., Gratton, M., Pettarin, V. et al. (2017). Recycling of waste tire rubber: microwave devulcanization and incorporation in a thermoset resin. *Waste Management, 60(12),* 471–481. DOI 10.1016/j.wasman.2016.10.051.
11. Gopi, S., Pius, A., Kargl, R., Kleinschek, K. S., Thomas, S. (2019). Fabrication of cellulose acetate/chitosan blend films as efficient adsorbent for anionic water pollutants. *Polymer Bulletin, 76(3),* 1557–1571. DOI 10.1007/s00289-018-2467-y.
12. Formela, K., Haponiuk, J. T. (2014). Curing characteristics, mechanical properties and morphology of butyl rubber filled with ground tire rubber (GTR). *Iranian Polymer Journal, 23(3),* 185–194. DOI 10.1007/s13726-013-0214-7.
13. Ramarad, S., Khalidm, M., Ratnam, C. T., Chuah, A. L., Rashmi, W. (2015). Waste tire rubber in polymer blends: a review on the evolution, properties and future. *Progress in Materials Science, 72,* 100–140. DOI 10.1016/j.pmatsci.2015.02.004.
14. Shen, M., Liu, J., Xin, Z. X. (2019). Mechanical properties of rubber sheets produced by direct molding of ground rubber tire powder. *Journal of Macromolecular Science, Part B, 58(1),* 16–27. DOI 10.1080/00222348.2018.1449798.
15. Wu, W. L., Zhang, J. (2012). Preparation and characterization of environment friendly used rubber powder modified pulp sediments composites. *Iranian Polymer Journal, 21(11),* 763–769. DOI 10.1007/s13726-012-0083-5.
16. Gopi, S., Balakrishnan, P., Pius, A., Thomasbc, S. (2017). Chitin nanowhisker (ChNW)-functionalized electrospun PVDF membrane for enhanced removal of Indigo carmine. *Carbohydrate Polymers, 165,* 115–122. DOI 10.1016/j.carbpol.2017.02.046.
17. Qing, Q., Zhou, L., Guo, Q., Gao, X. H., Zhang, Y. et al. (2017). Mild alkaline presoaking and organosolv pretreatment of corn stover and their impacts on corn stover composition, structure, and digestibility. *Bioresource Technology, 233,* 284–290. DOI 10.1016/j.biortech.2017.02.106.
18. Gopi, S., Balakrishnan, P., Divya, C., Valic, S., GovorcinBajsic, E. et al. (2017). Facile synthesis of chitin nanocrystals decorated on 3D cellulose aerogels as a new multi-functional material for waste water treatment with enhanced anti-bacterial and anti-oxidant properties. *New Journal of Chemistry, 42(21),* 12746–12755. DOI 10.1039/C7NJ02392H.
19. Xu, J. Y., Krietemeyer, E. F., Boddu, V. M., Liu, S. X., Liu, W. C. (2018). Production and characterization of cellulose nanofibril (CNF) from agricultural waste corn stover. *Carbohydrate Polymers, 192,* 202–207. DOI 10.1016/j.carbpol.2018.03.017.
20. Wu, W. L., Zuo, H. T. (2016). Used tire rubber powder/plant cellulose composites treated with coupling agent. *Cellulose, 23(3),* 1939–1947. DOI 10.1007/s10570-016-0952-8.